

## EVOLUTION OF THE ACCRETION STRUCTURE IN THE SYMBIOTIC BINARY BF CYGNI DURING ITS LAST OPTICAL OUTBURST BEGAN IN 2006

NIKOLAI A. TOMOV and MIMA T. TOMOVA

*Institute of Astronomy and National Astronomical Observatory,  
Bulgarian Academy of Sciences,  
BG-4700 Smolyan, POBox 136*

E-mail: tomov@astro.bas.bg, mtomova@astro.bas.bg

**Abstract:** The last optical eruption of the symbiotic eclipsing binary BF Cyg began in 2006 and continues up to the present time. In 2006 its brightness rose sharply reaching a maximum and after that gradually decreased reaching a minimum in 2014. After that it rose at two times again - in the beginning of 2015 and 2017. Its orbital photometric minima determined by eclipses were seen during this eruption. The evolution of the accretion structure surrounding the compact object and changing the depth of the orbital minimum is investigated on the basis of a broad band UBVR<sub>C</sub>I<sub>C</sub> photometric data and high resolution spectra in the range of the Balmer line H $\alpha$ . The parameters of this structure are determined at the times of the photometric orbital minima.

### 1. INTRODUCTION

The symbiotic system BF Cyg is an eclipsing binary and the eclipses are observed in its both states the quiescent and active ones. Its photometric orbital minimum is due to both an eclipse of the compact companion and an occultation of the circumbinary nebula (Tomov et al. 2015, hereafter Paper I). The last period of its activity began in 2006 and continues up to now. In 2006 the brightness increased sharply reaching a maximum. This high state was kept till 2008 and after that time the brightness slowly weakened and reached a minimal value in 2014. Four orbital minima were observed in this period. The depth of the orbital minimum changes. The second minimum is much shallower than the first one and after the second minimum the depth increases, the third minimum is deeper than the second one and the fourth – deeper than the third one (Skopal et al. 2015b). At one time between the first and second minima, since June 2009, satellite components of Balmer lines with a velocity of 300–400 km s<sup>-1</sup>, indicating high velocity bipolar collimated outflow, appeared in the spectrum and disappeared in

the end of 2012. In 2013 their velocity was much lower. A new activity of BF Cyg developed in the end of 2014 and since March 2015 the satellite components restored (Skopal et al. 2015a). The system was in its fifth orbital minimum in March 2016. The satellite components were interpreted in the framework of the model of a collimated stellar wind coming from the outbursting compact companion (Tomov et al. 2014).

In this work, we analyse the optical light curves of BF Cyg during its outburst begun in 2006 with the aim to propose one quantitative interpretation of the change of the depth of the orbital minimum (eclipse) in the framework of the same model. In this way we will trace the evolution of the disc-shaped structure surrounding the compact object which will give useful information for the future development of the models. Our final aim is to suggest a complete interpretation of the behaviour of the optical light of BF Cyg during its outburst after 2006.

For our consideration we will use the ephemeris of Fekel et al. (2001)

$$JD(\text{Min}) = 2451395.2^d + 757.2^d \times E,$$

where the eclipse of the compact object, occurring at the time of the inferior conjunction of the giant, is at zero phase.

## **2. BEHAVIOUR OF THE OPTICAL LIGHT AFTER THE FIRST LIGHT MAXIMUM**

After the first maximum in 2006 the light of BF Cyg decreases in different way compared to the next maxima (Fig. 1 in Paper I). Initially the U light falls steeply at about one magnitude. In our view it is most probably due to decrease of the mass-loss rate of the outbursting component which moves the level of the observed photosphere back to the star and redistributes the continuum emission from longer wavelengths towards the UV region. After the initial steeply fall the light begins to decrease more slowly and the basic reason for this decrease is the occultation of the circumbinary nebula. Assuming a decrease of the mass-loss rate, a part of the ejected material can remain within the gravitational potential of the compact object and begin to accrete (Tomov et al. 2014). Observational indication of the increase of the mass-loss rate can be an appearance of absorption component of the spectral lines. During the rise of the light to the second maximum the mass-loss rate was probably increased as proposed by the spectral data of Siviero et al. (2012). Strong P Cyg components of some Balmer and metal lines appeared after 2008 February 10. The light reached its second maximum at the end of 2008. Some time after that the Balmer lines acquired satellite components indicating bipolar collimated outflow (Skopal et al. 2013).

## **3. INTERPRETATION**

A scenario to interpret the spectrum of Z And during its 2000 – 2013 active phase involving two stages of the evolution of the outbursting compact object was presented in the works of Tomov et al. (2012, 2014). It is supposed that there is

geometrically thin disc from wind accretion surrounding the compact object in the system in its quiescence and during the first outburst of the active phase. At the end of the first outburst some part of the ejected material accretes again and because of conservation of its initial angular momentum falls into the disc. Thus one extended disc-like envelope covering the disc forms, which locates at a greater distance from the orbital plane than the accretion disc itself. In such a way the second stage of the evolution of the outbursting object begins, which is related to the following outbursts of the active phase. During the following outbursts the envelope can collimate the outflowing material and bipolar collimated outflow (collimated stellar wind) from the outbursting object can form.

The decrease of the depth of the orbital minimum implies an increase of the emission of the uneclipsed geometrical structure of the compact object. We suppose that a thin accretion disc from wind accretion has initially existed in the system BF Cyg and an extended disc-like envelope has formed after that as a result of decrease of the mass-loss rate and accretion of material from the potential well of the compact object in the period between the first and second orbital minima. We suppose that this envelope has collimated the stellar wind later. Some part of it is not eclipsed during the second and following minima determining their smaller depth. The emission of the jets is negligible (Paper I).

Our aim is to calculate the  $UBVR_{CIC}$  emission of such a model structure and to compare it with the observed residual of the depths of each minimum and the first minimum. If the model emission (the uneclipsed part of the envelope) is close to the observed residual, we can conclude that the formation of a disc-like envelope collimating the stellar wind of the compact object is a possible reason for both the appearance of the satellite components of the spectral lines and change of the depth of the orbital minimum of BF Cyg. After the third minimum the system's brightness fades and the depth of the orbital minimum increases again. We suppose that former is probably due to decrease of the optical flux of the outbursting object and destruction of the envelope and the latter – to destruction of the envelope only.

Gas dynamical modeling shows that a disc from wind accretion with a typical radius of  $50 - 60 R_{\odot}$  and a mass of  $5 \times 10^{-7} M_{\odot}$  exists in one binary system with parameters close to those of Z And in its quiescent state (Bisikalo et al. 2002; Tomov et al. 2010, 2011) During the outburst the wind of the compact object “strips” the disc and ejects some part of its mass. At the end of the outburst some part of the ejected mass locates in the potential well of the compact object. After the cessation of the wind it begins to accrete again creating an extended disc-like envelope with a mass smaller than the mass of the initial accretion disc.

The system BF Cyg has parameters very close to those of Z And – orbital period, masses of the components and mass-loss rate of the cool giant (Fekel et al. 2001). Then we suppose that a disc from accretion of a stellar wind with a size and a mass close to that in the system Z And exists in BF Cyg in its quiescent state. During the outburst the newly appeared disc-like envelope should have smaller mass (Paper I).

#### 4. BEHAVIOUR OF THE OPTICAL LIGHT AFTER THE FOURTH ORBITAL MINIMUM

An other activity of the compact object developed at the end of 2014, after the fourth orbital minimum, and the brightness began to grow reaching a maximum in February – March 2015 (Skopal et al. 2015a). The behaviour of the line spectrum reminded that in 2008–2009. In January 2015 the He I and Na I lines had P Cyg absorptions (Munari et al. 2015), and since March satellite  $H\alpha$  components appeared in the spectrum (Skopal et al. 2015a). In this way the  $H\alpha$  profile in July – August 2015 (Fig. 1) was very close to the profile in June – October 2009, containing a red emission satellite component with a velocity of about  $300 \text{ km s}^{-1}$ , which shows that a collimation mechanism with the same efficiency has probably begun to act in the system in 2015 (Tomov et al. 2018, hereafter Paper III). That is why, by analogy with the period between the first and second orbital minima, we supposed that as a result of a decrease of the mass-loss rate of the outbursting compact object prior to the fourth orbital minimum and accretion of material from its potential well, the disc-like envelope has restored in the time between the fourth and fifth minima on the basis of its remnant from 2014 (see Section 6).

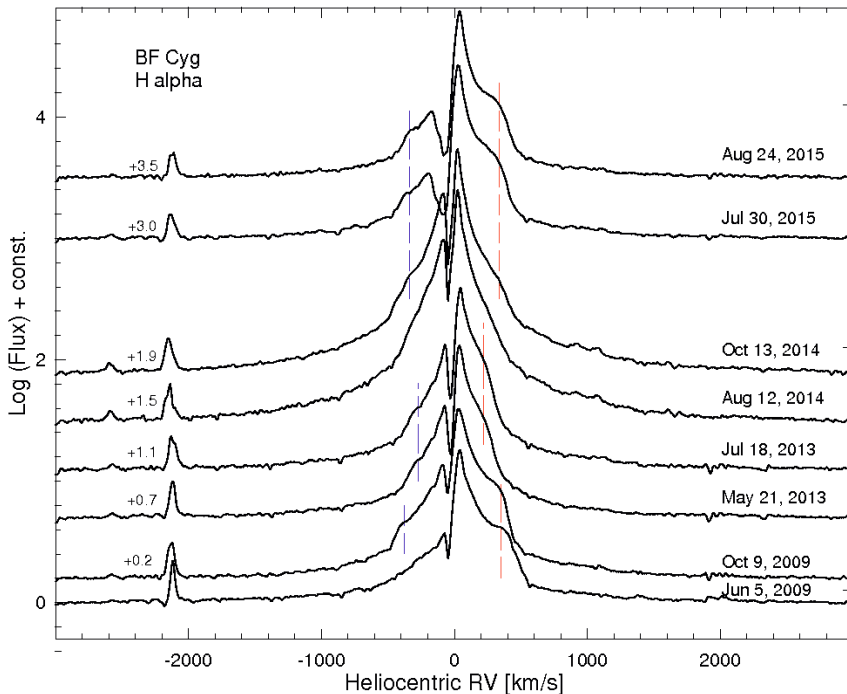


**Figure 1:** The  $H\alpha$  line profile in 2009, 2013, 2014 and 2015.

## 5. ANALYSIS OF THE CONTINUUM ENERGY DISTRIBUTION

### 5.1. UBVR<sub>C</sub>I<sub>C</sub> data used

In order to determine the parameters of the disc-like envelope at the times of the second (Dec. 13, 2009), third (Jan. 23, 2012), fourth (Feb. 11, 2014) and fifth (March 22, 2016) orbital minima it is necessary to have an estimate of the emission measure of the circumbinary nebula of BF Cyg, since it is an upper limit of the emission measure of the disc-like envelope (Tomov et al. 2017, hereafter Paper II). The greatest part of the circumbinary nebula is occulted at the time of the orbital minimum and that is why we estimated its emission measure at the time of its preceding orbital maximum although the nebular emission decreases with time. The brightness maximum on Feb. 26, 2015 is very close to the orbital maximum, which precedes the fifth orbital minimum on March 22, 2016 and we estimated the emission measure for the time of Feb. 26, 2015. In this way we needed in photometric data at the times of the photometric minima and their preceding maxima as well when the occulted part of the nebula is the smallest. We used photometric UBVR<sub>C</sub>I<sub>C</sub> data from the works of Skopal et al. (2012, 2015b, 2017). The continuum fluxes were calculated with use of the calibration data of Mihailov (1973). Unfortunately we were not provided with spectral data in the UB<sub>V</sub> range and that is why the U flux was not corrected for the energy distribution of BF Cyg in the region of the Balmer jump and, moreover, the UB<sub>V</sub> fluxes were not corrected for the emission lines. All fluxes were corrected for the interstellar reddening  $E(B-V) = 0.35$  (Skopal 2005) according to Cardelli et al. (1989) and are listed in Table 1.

**Table 1:** Dereddened fluxes of BF Cyg in units of  $10^{-12}$  erg cm<sup>-2</sup> s<sup>-1</sup> Å<sup>-1</sup> with their inner uncertainties at the times of the light minima and maxima under consideration.

| Extremum | Date           | $F_U$       | $F_B$       | $F_V$       | $F_{R_C}$   | $F_{I_C}$   |
|----------|----------------|-------------|-------------|-------------|-------------|-------------|
| Min 1    | Dec. 16, 2007  | 0.720±0.037 | 0.533±0.015 | 0.367±0.011 | 0.330±0.009 | 0.291±0.009 |
| Min 2    | Dec. 13, 2009  | 1.375±0.065 | 1.522±0.044 | 0.883±0.025 | 0.613±0.017 | 0.511±0.015 |
| Max 3    | Oct. 30, 2010  | 2.877±0.133 | 3.004±0.083 | 1.758±0.048 | 1.034±0.029 | 0.629±0.018 |
| Min 3    | Jan. 23, 2012  | 1.316±0.060 | 1.373±0.038 | 0.804±0.022 | 0.543±0.015 | 0.379±0.010 |
| Max 4    | Jan. 07, 2013  | 2.287±0.106 | 2.078±0.056 | 1.334±0.036 | 0.860±0.024 | 0.601±0.017 |
| Min 4    | Feb. 11, 2014  | 0.830±0.038 | 0.754±0.021 | 0.556±0.016 | 0.412±0.011 | 0.346±0.010 |
|          | Feb. 26, 2015  | 3.461±0.159 | 3.448±0.096 | 1.841±0.050 | 1.083±0.030 | 0.756±0.020 |
| Min 5    | March 22, 2016 | 0.830±0.038 | 0.907±0.025 | 0.556±0.016 | 0.376±0.010 | 0.330±0.009 |

### 5.2. The analysis

To estimate the emission measure of the circumbinary nebula we should analyse the continuum of the system to determine the basic parameters of its components (Paper II). The continuum flux of the giant was determined in the work of Skopal et al (2015b). It is known in this case, and we should determine

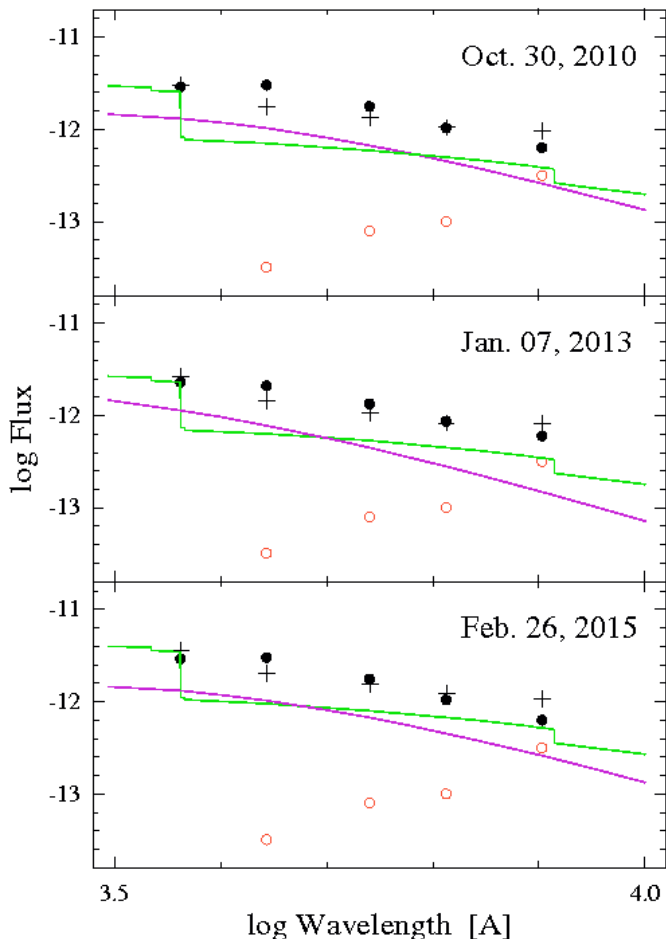


**Figure 2:** Spectral energy distribution of BF Cyg in the UBVR<sub>cIc</sub> range at the times of third (Oct. 30, 2010) and fourth (Jan. 7, 2013) orbital maxima after 2006 and the light maximum on Feb. 26, 2015. The points indicate the observed fluxes. The lines represent the black body and nebular continua and the circles – the fluxes of the giant. The crosses represent the resulting fluxes.

only the continua of the outbursting compact object and circumbinary nebula. We subtracted the UBVR<sub>cIc</sub> fluxes of the giant from the observed fluxes and approximated their residuals with a nebular continuum and black body emission. In order to approximate the data with a nebular continuum it is necessary to know the dominant ionization state of helium in the nebula. Our unpublished high resolution data do not show presence of the line He II 4686 in the spectrum of BF Cyg. Then, we assume that helium is singly ionized and the nebular continuum is emitted by hydrogen and neutral helium. To calculate the fluxes we used the formula described in Paper I about the continuum flux determined by recombinations and free-free transitions. We used continuum emission coefficients

from the paper of Ferland (1980) and the book of Pottasch (1984). We took the arithmetical mean of the hydrogen coefficient on both sides of the Balmer limit at the wavelength of the U band, a helium abundance of 0.1 (Vogel & Nussbaumer 1994) and a distance to the system of 3.8 kpc (Skopal 2005). In this way we approximated the observed fluxes at the times of third (Oct. 30, 2010) and fourth (Jan. 7, 2013) (Table 1) orbital maxima and on Feb. 26, 2015 with a nebular continuum with the same electron temperature of about 30000 K, that was obtained in the work of Skopal et al (2015b) for Oct. 23, 2008 at the time of the second maximum. For the time of the third maximum we obtained an emission measure  $n_e^2V = (2.00 \pm 0.15) \times 10^{61} \text{ cm}^{-3}$ , for the time of the fourth one  $n_e^2V = (1.80 \pm 0.12) \times 10^{61} \text{ cm}^{-3}$  and for Feb. 26, 2015 –  $n_e^2V = (2.70 \pm 0.17) \times 10^{61} \text{ cm}^{-3}$ . In addition the observed fluxes were approximated with black body emission with radius  $R = 18.0 \pm 2.0 R_\odot$  and  $T_{\text{eff}} = 10000 \pm 500 \text{ K}$  for the time of the third maximum,  $R = 10.5 \pm 1.0 R_\odot$  and  $T_{\text{eff}} = 13000 \pm 500 \text{ K}$  for the time of the fourth one and  $R = 18.0 \pm 2.2 R_\odot$  and  $T_{\text{eff}} = 10000 \pm 500 \text{ K}$  for Feb. 26, 2015 respectively. The spectral energy distribution for each time of maximum is shown in Fig. 2. Moreover, we established that the observed fluxes on Oct. 23, 2008 are really well approximated with a warm photosphere with  $R = 25 R_\odot$  and  $T_{\text{eff}} = 8500 \text{ K}$  as well as with a nebular emission with an emission measure of about  $2.6 \times 10^{61} \text{ cm}^{-3}$ , obtained in the work of Skopal et al. (2015b), but if the dominant ionization state of helium in the nebula is singly ionized, the continuum of the cool component is better approximated with the giant's photosphere with  $R = 150 R_\odot$  and  $T_{\text{eff}} = 3400 \text{ K}$  used in the work of Skopal (2005).

## 6. PARAMETERS OF THE DISC-LIKE ENVELOPE

When determining the parameters of the disc-like envelope we used a binary separation of BF Cyg of  $492 R_\odot$  resulting from the orbital solution of Fekel et al. (2001), a radius of the cool giant  $R = 150 R_\odot$  according to Skopal (2005) and an orbit inclination of  $75^\circ$  according to Skopal et al. (1997) and Fekel et al. (2001). Moreover, we supposed that the shape of the disc-like envelope is close to cylindrical ring (torus).

For the time of the second orbital minimum on Dec. 13, 2009 we accepted an inner radius of the disc-like envelope equal to the radius of the pseudophotosphere of the outbursting compact object on 2008 October 23 according to Skopal et al. (2015b), an outer radius very close to the mean size of the Roche lobe of the compact object, a height of  $170 R_\odot$  and a mass of the envelope of  $3.5 \times 10^{-7} M_\odot$ . Its mean density is thus  $7.5 \times 10^{10} \text{ cm}^{-3}$  (Table 2). With a radius of the giant of  $150 R_\odot$  about a half of the volume of the disc-like envelope will be visible during the eclipse at orbital phase 0.0 (Paper I). We will calculate the emission of the unclipped part of the envelope at this phase and will compare it with the observed residual of the depths of the first and second orbital minima in the photometric bands UBVR<sub>C</sub>I<sub>C</sub>. We accepted an electron temperature in the emitting region  $T_e = 30000 \text{ K}$  equal to the mean temperature in the nebula according to Skopal et al.

(2015b). The fluxes and emission measure of the whole circumbinary nebula, our model envelope and its uneclipsed part at orbital phase 0.0 are presented in Table 3. The emission measure of the nebula was taken from Skopal et al. (2015b) and its fluxes were calculated by us. The quiescent emission measure of BF Cyg at a phase very close to the orbital photometric maximum is  $3.1 \times 10^{60} \text{ cm}^{-3}$  (Skopal 2005) and on 2008 October 23 –  $2.6 \times 10^{61} \text{ cm}^{-3}$  (Skopal et al. 2015b). Its increase is thus  $2.3 \times 10^{61} \text{ cm}^{-3}$ . Then it appears that the emission measure of the envelope of  $2.2 \times 10^{61} \text{ cm}^{-3}$  is almost equal to this increase.

**Table 2:** Parameters of the disc-like envelope.

|                                | Minimum 2             | Minimum 3             | Minimum 4                 | Minimum 5             |
|--------------------------------|-----------------------|-----------------------|---------------------------|-----------------------|
| $R_{in}$ [ $R_{\odot}$ ]       | 25                    | 25                    | ...                       | 18                    |
| $R_{out}$ [ $R_{\odot}$ ]      | 150                   | 150                   | ...                       | $93 \div 78$          |
| $H$ [ $R_{\odot}$ ]            | 170                   | 130                   | ...                       | $90 \div 126$         |
| $M$ [ $M_{\odot}$ ]            | $3.5 \times 10^{-7}$  | $2.7 \times 10^{-7}$  | ...                       | $0.8 \times 10^{-7}$  |
| $n_e$ [ $\text{cm}^{-3}$ ]     | $7.5 \times 10^{10}$  | $7.5 \times 10^{10}$  | ...                       | $7.5 \times 10^{10}$  |
| $n_e^2 V$ [ $\text{cm}^{-3}$ ] | $2.21 \times 10^{61}$ | $1.70 \times 10^{61}$ | $(0.30 \times 10^{61})^a$ | $0.48 \times 10^{61}$ |

<sup>a</sup> The emission measure of the uneclipsed part

**Table 3:** UBVR<sub>C</sub>I<sub>C</sub> continuum fluxes and emission measure of the different regions in the circumbinary nebula. The fluxes are in units of  $10^{-12} \text{ erg cm}^{-2} \text{ s}^{-1} \text{ \AA}^{-1}$  and emission measure in  $10^{61} \text{ cm}^{-3}$ .

| Min            | Emitting region              | $F_U$             | $F_B$             | $F_V$             | $F_{RC}$          | $F_{IC}$          | $n_e^2 V$         |
|----------------|------------------------------|-------------------|-------------------|-------------------|-------------------|-------------------|-------------------|
| 2 <sup>a</sup> | Whole nebula                 | 2.184             | 0.913             | 0.768             | 0.647             | 0.491             | 2.60 <sup>b</sup> |
|                | Disc-like envelope           | 1.856             | 0.776             | 0.653             | 0.550             | 0.417             | 2.21              |
|                | Uneclipsed part              | 0.928             | 0.388             | 0.327             | 0.275             | 0.208             | 1.10              |
|                | Residual of the depths $r^c$ | $0.655 \pm 0.075$ | $0.989 \pm 0.046$ | $0.516 \pm 0.027$ | $0.283 \pm 0.019$ | $0.220 \pm 0.017$ |                   |
|                |                              | 42                | -61               | -37               | -3                | -5                |                   |
| 3              | Whole nebula                 | 1.680             | 0.702             | 0.591             | 0.498             | 0.377             | 2.00              |
|                | Disc-like envelope           | 1.428             | 0.596             | 0.502             | 0.424             | 0.320             | 1.70              |
|                | Uneclipsed part              | 0.714             | 0.298             | 0.251             | 0.212             | 0.160             | 0.85              |
|                | Residual of the depths $r^c$ | $0.596 \pm 0.070$ | $0.840 \pm 0.041$ | $0.437 \pm 0.024$ | $0.213 \pm 0.017$ | $0.088 \pm 0.013$ |                   |
|                |                              | 20                | -64               | -43               | 0                 | 85                |                   |
| 4              | Whole nebula                 | 1.512             | 0.632             | 0.532             | 0.448             | 0.346             | 1.80              |
|                | Disc-like envelope           | 0.504             | 0.210             | 0.178             | 0.150             | 0.116             | 0.60              |
|                | Uneclipsed part              | 0.252             | 0.103             | 0.089             | 0.075             | 0.058             | 0.30              |
|                | Residual of the depths $r^c$ | $0.110 \pm 0.053$ | $0.221 \pm 0.026$ | $0.189 \pm 0.019$ | $0.082 \pm 0.014$ | $0.055 \pm 0.013$ |                   |
|                |                              | 120               | -52               | -53               | -8                | 5                 |                   |
| 5              | Whole nebula                 | 2.268             | 0.948             | 0.798             | 0.672             | 0.509             | 2.70              |
|                | Disc-like envelope           | 0.404             | 0.168             | 0.142             | 0.120             | 0.092             | 0.48              |
|                | Uneclipsed part              | 0.202             | 0.084             | 0.071             | 0.060             | 0.046             | 0.24              |
|                | Residual of the depths $r^c$ | $0.110 \pm 0.053$ | $0.374 \pm 0.029$ | $0.189 \pm 0.019$ | $0.046 \pm 0.013$ | $0.039 \pm 0.013$ |                   |
|                |                              | 84                | -78               | -62               | 30                | 18                |                   |

<sup>a</sup>The data for this minimum are from the work of Tomov et al. (2015) and are included in the Table for comparison.

<sup>b</sup>The data are for 2008 October 23 in the work of Skopal et al. (2015).

<sup>c</sup> $r = (U - R)/R$  in per cent; U – Uneclipsed part, R – Residual of the depths.

The spectral data of Skopal et al. (2013, 2015b) as well as our spectra in Fig. 1 show that the velocity of the satellite components of Balmer lines of BF Cyg was of about  $400 \text{ km s}^{-1}$  in the period from June 2009 to the end of 2012 and after the beginning of 2013 it decreased. This means that the collimating mechanism preserved until the end of 2012 and changed after that. For this reason we suppose that the parameters of the disc-like envelope at the time of the third orbital minimum have been close to those in the second one, and at least some of these parameters at the time of the fourth minimum have been different from those in second and third ones (Paper II). The results of gas dynamical modeling show that the stellar wind of the compact object destroys its accretion disc – the wind “strips” the disc ejecting some part of its mass and moreover, it can increase its inner radius (Tomov et al. 2010, 2011). The ability of one disc shaped structure to collimate the outflowing gas depends strongly on its inner radius. Since the velocity of the satellite components during the third minimum was the same like in the second one, we adopted the same inner radius and an outer radius very close



again to the size of the Roche lobe of the compact object. We adopted a mean density of the envelope of  $7.5 \times 10^{10} \text{ cm}^{-3}$ , the same as for the second minimum. As for the height of the disc-like envelope, we supposed that it has decreased little, so that with the binary separation, giant's radius and orbit inclination accepted by us, the shadow of the giant passes through the lateral area of the cylinder. When we considered the second orbital minimum we concluded that the eclipsed and uneclipsed parts of the envelope are approximately equal.

We approximated the residual of the depths of the first and third orbital minima in the photometric bands  $UBVR_C I_C$  with a nebular emission with  $T_e = (30000 \pm 3000) \text{ K}$  and an emission measure of  $(0.85 \pm 0.08) \times 10^{61} \text{ cm}^{-3}$ . This is the emission measure of the uneclipsed part of the envelope at phase 0.0 and according to our conclusion the emission measure of the whole envelope should be  $(1.70 \pm 0.16) \times 10^{61} \text{ cm}^{-3}$  (Table 3). Having the emission measure and mean density of the envelope we obtained its mass  $M = 2.7 \times 10^{-7} M_\odot$ . Based on this mass and the two radii, we obtained its height of  $130 R_\odot$  (Table 2). With this height and the binary separation, giant's radius and orbit inclination accepted by us, the shadow of the giant will really pass through the lateral area of the cylinder, which means that our supposition is true.

The emission measure of the circumbinary nebula at the time of the third maximum, obtained by us, is  $(2.00 \pm 0.15) \times 10^{61} \text{ cm}^{-3}$ . The quiescent emission measure of BF Cyg at phase close to the orbital maximum is  $3.1 \times 10^{60} \text{ cm}^{-3}$  (Skopal 2005). It appears that the emission measure of the disc-like envelope is equal to their residual like in the case of the second orbital minimum (Table 3).

An essential feature of the behaviour of the line spectrum of BF Cyg is that from the beginning of 2013 the velocity of the satellite components decreased (Fig. 1), which means that the system has changed, so that its ability to collimate the gas was decreased. Besides the height, it is possible that the inner radius and consequently the mean density of the envelope have changed as well (Paper II). These parameters cannot be estimated from observation and for the time of the fourth minimum we can obtain only the emission measure of the uneclipsed part of the envelope at phase 0.0. We approximated the residual of the depths of the first and fourth orbital minima with nebular emission with  $T_e = (30000 \pm 3000) \text{ K}$  and an emission measure of  $(0.30 \pm 0.06) \times 10^{61} \text{ cm}^{-3}$ . This result shows that at the time of the fourth minimum the emission measure of the envelope is not comparable to that of the whole nebula but is much smaller (see Table 3).

The residual of the depths of the first and fifth orbital minima in the photometric bands  $UBVR_C I_C$  was approximated with a nebular emission with  $T_e = (30000 \pm 3000) \text{ K}$  and an emission measure  $n_e^2 V = (0.24 \pm 0.07) \times 10^{61} \text{ cm}^{-3}$ , which should be related to the uneclipsed part of the envelope at phase 0.0. Then the emission measure of the whole envelope amounts to  $(0.48 \pm 0.14) \times 10^{61} \text{ cm}^{-3}$  (Table 3). With the density used by us we obtained a volume of the envelope of  $8.53 \times 10^{38} \text{ cm}^3$  and a mass  $M \sim 0.8 \times 10^{-7} M_\odot$ . The inner radius of the envelope  $R_{in}$  is not smaller than the radius of the observed photosphere of the outbursting compact object and we will adopt the radius of this photosphere for the inner

radius as we proceeded in the cases of the second and third orbital minima. In regard to the outer radius  $R_{\text{out}}$  and the height  $H$ , we can not determine any of them from observation. The emission measure of the envelope at the times of the second and third orbital minima was great and its mean density to be close to  $10^{10} \text{ cm}^{-3}$ , the outer radius had to be equal to the radius of the Roche lobe. At the time of the fifth minimum the emission measure is smaller and the outer radius is probably smaller than the Roche lobe. To determine this radius we supposed that the ratio  $H/R_{\text{in}}$  is within the interval 5–7, since it was in approximately the same interval at the times of the second and third orbital minima, when the  $H\alpha$  profile contained satellite components with the same velocity as in 2015. Using this ratio and an inner radius  $R_{\text{in}} = 18 R_{\odot}$ , we obtained that the outer radius  $R_{\text{out}}$  and the height  $H$  are in the intervals 93–78  $R_{\odot}$  and 90–126  $R_{\odot}$  (Table 2). With these values the shadow of the giant will really pass through the lateral area of the cylinder and our supposition turned out to be true. The mass and sizes of the disc-like envelope obtained show that it is smaller than at the times of the second and third minima. Its mass and sizes, however, are also close to those predicted by the gas-dynamical modeling (Bisikalo et al. 2002; Tomov et al. 2010, 2011), which means that it can be considered as the accretion structure which collimates the gas at the time of the fifth minimum (Paper III).

## 7. CONCLUSIONS

We interpreted the variability of the optical brightness of the symbiotic binary BF Cyg during its last outburst begun in 2006 with the evolution of an accretion structure surrounding the outbursting compact object. This structure is related to a disk-like envelope appeared around the initial accretion disk as a result of diminution of the mass-loss rate of the compact object after the first light maximum and accretion of material from its potential well in the time between the first and second orbital minima in December 2007 and December 2009. The uneclipsed part of the disk-like envelope is responsible for the decrease of the depth of the orbital minimum. The envelope is destroyed by the stellar wind of the outbursting object and after the second orbital minimum the depth of the minimum increases again. In the period from the beginning of the outburst to 2014 the optical brightness of the system decreases for two reasons: a diminution of the flux of the compact object because of moving the level of its pseudophotosphere back to the star and redistribution of its continuum from longer wavelengths towards the UV region and destruction of the envelope. In the period between the fourth and fifth orbital minima in February 2014 and March 2016 the disk-like envelope restores from its remnant as a result of accretion of material from the potential well of the compact object again and satellite components with a velocity close to their velocity in 2009–2012 begin to be observed.

We supposed that the shape of the envelope is close to a torus and obtained its parameters for each time of orbital minimum adopting the next parameters of the system: a binary separation of 492  $R_{\odot}$ , an orbit inclination of  $75^{\circ}$  and a radius of

the cool giant  $R = 150 R_{\odot}$ . With these parameters about a half of the volume of the disk-like envelope is visible during the eclipse at orbital phase 0.0. We accepted a mean density of the envelope of  $7.5 \times 10^{10} \text{ cm}^{-3}$  and determined its inner and outer radii, height and mass. For an inner radius was accepted the radius of the observed photosphere (pseudophotosphere) of the outbursting compact object, which, from its side, was determined from analysis of the continuum energy distribution of the system BF Cyg in the range of the photometric bands  $UBVR_{cI_C}$ . The emitted by the uneclipsed part of the envelope  $UBVR_{cI_C}$  fluxes have been calculated and compared with the observed residual of the depths of each orbital minimum and the first one. It turned out that the model fluxes are in satisfactory agreement with the observed ones.

### Acknowledgments

This work was partially supported by the Bulgarian National Science Fund of the Ministry of Education and Science under grants DN 08-1/2016 and DN 18-13/2017.

### References

- Bisikalo D.V., Boyarchuk A.A., Kilpio E.Yu., Kuznetsov O.A.: 2002, *ARep*, **46**, 1022.  
 Cardelli J.A., Clayton G.C., Mathis G.C.: 1989, *AJ*, **345**, 245.  
 Fekel F.C., Hinkle K.H., Joyce R.R., Skrutskie M.F. : 2001, *AJ*, **121**, 2219.  
 Ferland G.J.: 1980, *PASP*, **92**, 596.  
 Mihailov A.A.: 1973, *Kurs astrofiziki i zvezdnoj astronomii*, Moscow, Nauka, (in Russian).  
 Munari U., Siviero A., Dallaporta S., et al.: 2015, *ATel* 7013.  
 Pottasch S.R.: 1984, *Planetary nebulae*, Dordrecht, Reidel.  
 Siviero A., Tamajo E., Lutz J., Wallerstein G., ANS Collaboration: 2012, *BaltA*, **21**, 188.  
 Skopal A.: 2005, *A&A*, **440**, 995.  
 Skopal A., Vittone A.A., Errico L., et al.: 1997, *MNRAS*, **292**, 703.  
 Skopal A., Shugarov S., Vanko M., et al.: 2012, *AN*, **333**, 242.  
 Skopal A., Tomov N.A., Tomova M.T.: 2013, *A&A*, **551**, L10.  
 Skopal A., Sekeráš M., Shugarov S., Pribulla T., Vanko M.: 2015a, *ATel* 7258.  
 Skopal A., Sekeráš M., Tomov N.A., Tomova M.T., Tarasova T.N., Wolf, M.: 2015b, *AcPol CTU Proc.* **2**, 277.  
 Skopal A., Sekeráš M., Shugarov S., Shagatova N.: 2017, *ATel* 10086.  
 Tomov N.A., Bisikalo D.V., Tomova M.T., Kilpio E.Yu.: 2010, *ARep*, **54**, 628.  
 Tomov N.A., Bisikalo D.V., Tomova M.T., Kilpio E.Yu.: 2011, *AIP Conf. Proc.*, **1356**, 35.  
 Tomov N.A., Tomova M.T., Bisikalo, D.V.: 2012, *BaltA*, **21**, 112.  
 Tomov N.A., Tomova M.T., Bisikalo D.V.: 2014, *AN*, **335**, 178.  
 Tomov N.A., Tomova M.T., Bisikalo D.V., 2015, *AN*, **336**, 690 (Paper I).  
 Tomov N.A., Tomova M.T., Bisikalo D.V., 2017, *Ap&SS*, **362**, 220 (Paper II).  
 Tomov N.A., Tomova M.T., Bisikalo D.V., 2018, submitted (Paper III).  
 Vogel M., Nussbaumer H.: 1994, *A&A*, **284**, 145.